Experimental study on the nucleate boiling heat transfer characteristics of a water-based multi-walled carbon nanotubes nanofluid in a confined space

XIA, Guodong, DU, Mo, CHENG, Lixin and WANG, Wei

Experimental study on the nucleate boiling heat transfer characteristics of a water-based multi-walled carbon nanotubes nanofluid in a confined space

Guodong Xia[a,*], Mo Du[a], Lixin Cheng[a,b], Wei Wang[a]

[a]*Key Laboratory of Enhanced Heat Transfer and Energy Conservation, Ministry of Education, College of Environmental and Energy Engineering, Beijing University of Technology, Beijing 100124, China*

[b]*Department of Engineering and Mathematics, Faculty of Arts, Computing, Engineering and Science, Sheffield Hallam University, City Campus, Howard Street, Sheffield, S1 1WB, UK*

Abstract: Experimental investigation of nucleate boiling heat transfer of a water-based multi-walled carbon nanotubes (MWCNTs) nanofluid in a confined space is presented in this study. First, the effects of four different surfactants on the stability of the nanofluids were investigated and the suitable surfactant gum acacia (GA) was selected for the boiling experiments. Then, the boiling experiments of the nanofluids with various volume fractions (0.005% - 0.2%) of the MWCNTs were conducted at a sub-atmospheric pressure of 1×10^{-3} Pa and the test heat fluxes are from 100 to 740 kW/m^2. Furthermore, GA with four different mass fractions was respectively dissolved in the nanofluids to investigate the effect of the GA concentration on the boiling heat transfer. The effects of the heat flux, the concentrations of the MWCNTs and surfactants, the bubble behaviors and the surface conditions after the boiling processes have been analyzed. The results show that the MWCNTs nanofluid can enhance boiling heat transfer as compared to the base fluid. This is mainly caused by the nanoparticles deposition on the boiling surface result in increasing the surface roughness and reducing surface contact angle. It is also found that addition of GA can inhibit the deposition of the nanoparticles but may reduce the boiling heat transfer coefficient of the nanofluids. According to the

experimental results, the maximum heat transfer coefficient enhancement ratio can reach 40.53%. It is also noticed that the heat transfer enhancement ratio decreases with increasing the heat flux at lower heat fluxes from 100 to 340 kW/m^2 while it increases with increasing the heat flux at higher fluxes from 340 to 740 kW/m^2. At the lower heat fluxes, the deposition layer increases the frequency of bubble formation and thus the boiling heat transfer is strengthened. While at the high heat fluxes, the increasing heat flux may strengthen the capability of the nanoparticles deposition and the disturbance of the nanoparticles and increase the enhancement ratio of heat transfer coefficient.

Keywords: nanofluids, MWCNTs, nucleate boiling, heat transfer, enhancement, mechanism

1. Introduction

As a new type of heat transfer medium, nanofluids have been attracting tremendous attention in the field of thermal science and engineering in recent years due to their high thermal conductivity, unique colloidal property and heat transfer behaviors [1-8]. Numerous researchers have conducted investigation into the heat transfer enhancement including single phase and phase change heat transfer using nanofluids [9-20]. In particular, the nucleate boiling heat transfer characteristics in confined spaces are of great interest to removing high heat flux in the microelectronic system, laser devices, green and highly efficient lighting with limited cooling spaces. Although a large number of researchers have investigated on the pool boiling heat transfer characteristics with plenty kinds of nanofluids in unconfined spaces, there lacks study of the characteristics of nucleate boiling heat transfer using the multi-walled carbon nanotubes (MWCNTs) nanofluid in confined spaces at sub-atmospheric pressures. Therefore, it is essential to conduct experimental investigation on the relevant topic.

Nanofluids which possess application prospects in the heat transfer field were firstly

proposed by Choi [1] in 1995. From then on, numerous studies of heat transfer of nanofluids have been conducted to understand and explore their fundamentals and applications. The suspension stability and thermal conduction mechanism of nanofluids were studied by Xuan et al. [2], Assael [3] and many other researchers [4, 5]. Hwang et al. [6] prepared four kinds of nanofluids using MWCNTs, CuO and SiO_2 nanoparticles. They found that the thermal conductivity of nanofluids was higher than its base fluid and the thermal conductivity of MWCNTs nanofluid was the highest than other nanofluids under the same concentration.

As a new research frontier, nanofluids two phase flow and thermal physics is the subject of growing concern [7, 8]. Investigation into the nanofluids phase change phenomena and complicated heat transfer mechanisms have intensively been performed over the past decade. Most researchers have found that the mechanisms of pool boiling heat transfer of nanofluids are different from those of conductive and convective heat transfer of nanofluids [11-13]. Yang and Maa [14] are possibly the first to conduct pool boiling experiments using nanofluids. Their experimental results have indicated that low concentrations of Al_2O_3 nanofluids with 50 nm diameter can enhance the nucleate pool boiling heat transfer. Xue et al. [15] studied the boiling curve, bubble pattern and contact angle of gum acacia (GA) solution and carbon nanotubes nanofluids. The results showed GA solution enhanced transition boiling heat transfer rate, since GA powder improved the wettability of water. In addition, the critical heat flux of nanofluids pronouncedly increases than that of GA solution due to the deposition of nanoparticles. Amiri et al. [16] performed some pool boiling experiments using carbon nanotubes nanofluid considering different functional groups of nanotubes. They investigated the pool boiling HTC of covalent nanofluids increases than that of deionized water, the heat transfer of non-covalent nanofluids became worse for the reason of the effect of heat resistance. Sarafraz et al. [17-19] study the pool boiling of the MWCNTs and Al_2O_3 nanofluids on several surfaces and conditions. About MWCNTs nanofluids, they found that the nucleate boiling of the nanofluids could still lead to

the particle deposition, but the micro-finned surfaces broke the deposition to enhance the nucleation site and thus the boiling heat transfer increasing. Shoghl et al. [20] studied the pool boiling heat transfer of nanofluids with ZnO, α-Al_2O_3 and MWCNTs. Their results indicate that the effects of boiling surface and properties of nanofluids to prove both of them may significantly influence the boiling heat transfer characteristics. For instance, the carbon nanotube-water nanofluids which improved the property of fluids and boiling surface characteristics could enhance the nucleate boiling heat transfer. Quite different results of nucleate boiling heat transfer with various surface conditions have been reported by researchers. Therefore, it is essential to explore and understand the various mechanisms governing the heat transfer processes.

According to the foregoing literature review, it is obvious that quite different results of boiling heat transfer with nanofluids and experimental conditions have been obtained. As pointed out by Cheng and Liu [7], there are still challenges to understand the boiling phenomena of nanofluids and their heat transfer mechanisms. Great effort should be made to achieve the complete and systematic knowledge in this aspect. In particular, it's still necessary to investigate and understand the heat transfer mechanisms through well designed and careful performed experiments and theoretical analysis.

Furthermore, the confined heat sink can be traced back to the ribbed radiator of CPU etc. In order to reduce the space and improve the heat efficiency of heat exchanger, flat plate heat pipe thermal spreader replaces the traditional radiator. The boiling in confined space condition just happens in this kind of heat pipe. Rops et al. [21] analyzed the nucleate boiling heat transfer on a spatially confined surface. They found that the depth of the boiling pot, the material of the bounding wall and the diameter of the inlet water supply didn't affect the enhancement of boiling heat transfer. Zhang et al. [22] reported an experimental investigation of phase-change phenomena in a small confined space. In the study, the boiling and condensation possessed

dramatically impacted each other and the bubbles were limited not only by the distance between boiling and condensation surface, but also by the condensation process. Liu and Yang [23] observed that the boiling heat transfer characteristics were affected by lots of factor in confined space, especially vapor blowing, liquid suction and vapor waving resistance. They also found the enhancement ratio of heat transfer coefficient reduced by the condition of decreasing boiling space or increasing heat flux. However, the study of boiling heat transfer using nanofluids in confined spaces at sub-atmospheric pressures is very limited in the literature so far. Using nanofluid as working fluid seems a promising method of improving the heat transfer performance. The study on the mechanism of boiling heat transfer in confined with nanofluids is helpful to the application of nanofluids. Therefore, it is necessary to conduct the relevant study in this aspect.

The objectives of this paper are to experimentally investigate the complicated nucleate boiling mechanisms of nanofluids in a confined space under a sub-atmospheric pressure condition. First, the technology used for preparation of nanofluids is described. Then, experiments of nucleate boiling heat transfer of the MWCNTs nanofluids were conducted in a confined space at a pressure of 1×10^{-3} Pa. The influences of heat flux, the concentration of nanofluids and surfactant on the heat transfer behaviors were presented. The scanning electron microscopy (SEM) photographs of boiling surfaces were used to analyze the modification by the deposition of nanoparticles. The roughness and contact angle of boiling surface and the visualization of the bubble behaviors were used to explain the boiling heat transfer mechanisms of the MWCNTs nanofluids.

2. Technology of the water-based MWCNTs nanofluid preparation

2.1. Characterization of the MWCNTs

The multi-walled carbon nanotube nanoparticles were manufactured by Beijing DK Nano

technology Co. Ltd utilizing the chemical vapor deposition method. The physical parameters of the MWCNTs are shown in Table 1. The MWCNTs have an outer diameter of 10-20 nm and an inner diameter of 5-10 nm. Their length is from 10 to 30 μm. The density of the MWCNTs is 2.1 g/cm^3 and its specific surface area is 200 m^2/g. The purity of the MWCNTs is larger than 98%. Figure 1(a) shows a transmission electron microscopy (TEM) photograph of the multiple carbon walls of a tubular structure of the MWCNTs at a scale of 20 nm. Figure 1(b) shows a SEM photograph of the MWCNTs at scale of 500 nm. It can be seen that the nanoparticles agglomerate and twine together. Therefore, it is necessary to scatter the nanoparticles using physical and chemical methods [24-26] at first when preparing the water-based MWCNTs nanofluids.

2.2. Technology for preparation of the water-based MWCNTs nanofluid

In this study, magnetic stirrer and ultrasonic oscillation were adopted to disperse the MWCNTs in the base fluid deionized water. In addition, some surfactants were added in the base fluid to prevent the second aggregation and suspend the MWCNTs stably for a long time. In general, one step method or two step method is used for the preparation of the nanofluids [27]. The two steps method was adopted to prepare the water-based MWCNTs nanofluids. The first step is to prepare the nanoparticles which have been manufactured. The surfactant is added into the base fluid and the solution is well mixed by stirring the solution with a magnetic stirrer for 5 minutes. Then the nanoparticles are added into the surfactant solution. After 5 minutes stirring with the magnetic stirrer, the nanofluid is then well mixed with an ultrasonic oscillation for 1 hour.

Selection of a surfactant was performed at first. Four different popular surfactants which have been used in the nanofluids preparation including cetyltrimethyl ammonium bromide (CTAB), polyvinyl pyrrolidone (PVP), sodium dodecyl benzene sulfonate (SDBS) and gum acacia (GA) were initially used in preparing the MWCNTs nanofluids. The surfactants were all

white particles and manufactured by Tianjin Fuchen Chemical Reagents Factory. The effects of surfactant on the stability of the nanofluids stability were studied through the static precipitation method. All the fresh prepared nanofluid samples with 0.1% volume concentrations of MWCNTs and four kinds of surfactants with 0.1% mass concentration looked similar in appearance, as shown in Fig. 2 (a). As is shown, the nanofluid with CTAB has foam at the liquid surface and the foam remains there for a long time. Foaming was found in the nanofluids with SDBS when prepared it, but it vanished quickly after standing a while. The nonion surfactants (PVP and GA) did not provide any foam. After standing for three months as shown in Fig. 2 (b), some obvious nanoparticles precipitation can be found in the nanofluids with the cation and anion surfactants (CTAB and SDBS). The nanofluids with the nonion surfactants have much better stability than cation and anion surfactants. Yazid et al. [28] pointed out that GA was frequently used as the surfactant to stabilize the carbon nanotubes in water. Our observation has confirmed their statement. Therefore, GA was chosen as the surfactant in preparing the water-based MWCNTs nanofluid used in the boiling experiments.

As mentioned above, stable dispersed nanofluids can be prepared adding GA with 0.1% mass concentration. Increasing the concentration of surfactant can explore the influence of the surfactant on boiling, so GA with four different mass concentrations of 0.1%, 0.3%, 0.5% and 0.7% was respectively dissolved in the base fluids. The MWCNTs of five different volume fractions of 0.005%, 0.01%, 0.05%, 0.1% and 0.2% were added into the base fluids with or without the surfactant. All the MWCNTs nanofluids with and without GA were prepared for the boiling experiments in the present study.

3. Experimental setup and experiment procedure

The experimental setup consists of an experimental rig, an assembled test section and a measurement system. The details of these are elaborated here in this section.

3.1 . Experimental rig

Figure 3 shows the schematic diagram of the experimental rig used for the nucleate boiling heat transfer experiments in a confined space. The experimental rig mainly includes a thermostatic water container (1), voltage regulator (2), cartridge heaters (3), a copper rod (4), insulation layer (5), a copper sheet (6), quartz window (7), pressure gauge (8), a vacuum pump (9), a high-speed video camera (10), a data acquisition instrument (11) and a PC (12). It consists of a boiling system, a condensation system, a visualization quartz window together with a high-speed video camera, a measurement system and a PC for storing the measured parameters.

The boiling system includes a test section, a copper rod, several cartridge heaters and a voltage regulator. Four cartridge heaters were assembled inside a copper rod which is tightly contacted with a flat test section. The cartridge heaters connected to a voltage regulator are used to generate heat through electrical resistance and transfer the heat through the copper rod to the test section to generate boiling processes. The voltage regulator is used to adjust the heat flux in the boiling experiments.

The condensation system comprises a condensation chamber, a copper sheet and a thermostatic water container. Water in the thermostatic container was maintained at a constant temperature of 12℃ and used to condensate the vapor generated in the test chamber. The vacuum device is used to remove the gas in the boiling test chamber before fill up the working fluid and maintain a sub-atmospheric pressure condition specified in the boiling experiments. The chamber wall between two copper sheets is made of a quartz window which is used for the visualization of the boiling process using the high-speed video camera.

Three T type thermocouples arranged along the axial direction of the copper rod are used to measure the local temperatures along the axis of the round copper rod. With the measured temperatures, the boiling surface temperature of the test section and heat flux can be calculated using one-dimensional linear heat conduction. The surface of the copper sheet was polished with

198 a 5000# sandpaper before the experiments. The data acquisition system is used to collect the
199 temperatures of three points on the top of the copper heater, the fluid temperature, the vapor
200 temperature in the test chamber and the operation pressure.

201 *3.2 . Test section*

202 Figure 4 shows the schematic diagram of the test section and the heating system. The
203 heating section is mainly composed of the copper sheet, the copper rod and four cartridge heaters
204 with a diameter of 8 mm. As is showed in Fig. 4, both sections of the upper and lower copper rod
205 are cylindrical and four cartridge heaters are symmetrically arranged at the lower end of the rod
206 to provide heat source for the boiling experiments. The maximum heat flux was adjusted to 750
207 kW/m^2 which does not reach critical heat flux as we focused on nucleate boiling heat transfer and
208 mechanisms in our study. The diameter of the upper copper rod is 20 mm, which has the same as
209 the diameter of the boiling surface. Three T type thermocouples are arranged along the axis of
210 the copper rod in the upper section of it to measure the local temperatures and then they are used
211 to calculate the heat flux and the temperature of boiling surface in the boiling experiments.
212 Thermal grease was used to connect the thermocouples and copper rod, so the contact resistance
213 could be neglected. In order to investigate the boiling heat transfer characteristics of the
214 MWCNTs nanofluids at sub-atmospheric pressure, the vacuum system is used to achieve the
215 desired test pressure of 1×10^{-3} Pa. The top surface of the copper rod connected to a horizontal
216 copper sheet which a thickness of only 0.3 mm. The thin sheet of copper has an excellent sealing
217 effect while can neglect horizontal heat conduction effectively because of its thin axial size.

218 *3.3 . Experimental procedure*

219 To conduct the boiling experiments, first, the vacuum system was run for more than 30
220 minutes to make the test chamber at a sub-atmospheric condition. Second, the working fluid was
221 pumped into the test chamber. Following this, the vacuum device was operated again to
222 discharge the dissolved gas escaped from the working fluid and an operation pressure of 1×10^{-3}

Pa was maintained in the test chamber for the boiling experiments. Finally, the condensation system, the circulating water system, the data acquisition system and the power supply was started in sequence. The voltage regulator was used to adjust the voltage at several values of 50 V, 70 V, 90 V, 100 V, 110 V, 120 V, and 130 V to generate different heat fluxes used for the test runs in the boiling experiments. After steady state was achieved for each test run, the measured parameters were taken by the data acquisition system and stored in the PC for further data reduction and analysis.

4. Data reduction methods and uncertainty analysis

4.1. Data reduction methods

With the measured parameters of local temperatures in the copper rod and the fluid temperature, the heat flux and boiling heat transfer coefficient may be calculated. The boiling heat transfer coefficient is calculated as:

$$h = \frac{q}{T_{\mathrm{w}} - T_{\mathrm{f}}} \tag{1}$$

where T_{w} is the wall surface temperature of the test section and T_{f} is the saturation temperature of the working fluid, (T_{w}-T_{f}) is the superheat degree and q is the heat flux.

It's not accurate to calculated heat flow by the voltage and current of the power supply due to a small amount of heat loss. Therefore, the heat flux would be obtained through steady state heat conduction along the axial direction of the copper rod, assuming one dimensional heat conduction, as

$$q = -\lambda \frac{\mathrm{d}T}{\mathrm{d}z} = -\lambda \cdot \frac{1}{2} \cdot \left(\frac{T_3 - T_2}{\Delta z_{3-2}} + \frac{T_2 - T_1}{\Delta z_{2-1}} \right) \tag{2}$$

where λ is the thermal conductivity of the copper heater, dT/dz is the average temperature gradient calculated according to the measured temperatures T_1, T_2, and T_3 as indicated in Fig. 4, z

is the axial distance between the two temperature measurement points. The calculated value of heat flux is slightly lower than the power supply within 7%.

The boiling surface temperature of the test section T_w is determined using one dimensional conduction heat transfer along the vertical direction of the copper heater as:

$$T_w = T_1 + \frac{dT}{dz}\Delta z_{w\text{-}1} = T_1 + \frac{1}{2}\times\left(\frac{T_3 - T_2}{\Delta z_{3-2}} + \frac{T_2 - T_1}{\Delta z_{2-1}}\right)\times 0.023 \quad (3)$$

To evaluate the enhancement of the nucleate boiling heat transfer of the nanofluids, the heat transfer coefficient enhancement ratio is defined as:

$$\eta = \frac{h_{nf} - h_{dw}}{h_{dw}} \times 100\% \quad (4)$$

where h_{nf} and h_{dw} are the boiling heat transfer coefficients of the MWCNTs nanofluids and the deionized water respectively.

4.2. Uncertainty analysis

The thermocouples were well calibrated before the experiments and the measured temperatures are accurate to ± 0.1 K. The measured pressure gauge is accurate to 0.25% and the distances between the two temperature measurement points are accurate to ± 0.1 mm. The accuracies of voltmeter and ammeter are ± 0.1V and ± 0.025A.

Using the methods of Kline and McClintock [29], the uncertainties of heat flux and heat transfer coefficient determined by Eqs. (1) and (2) may be analyzed as follows:

$$\frac{\Delta q}{q} = \sqrt{\left(\frac{\Delta\lambda}{\lambda}\right)^2 + \left(\frac{\Delta\delta T}{\delta T}\right)^2 + \left(\frac{\Delta\delta z}{\delta z}\right)^2} \quad (5)$$

$$\frac{\Delta h}{h} = \sqrt{\left(\frac{\delta q}{q}\right)^2 + \left(\frac{\Delta\delta T}{\delta T}\right)^2} \quad (6)$$

The uncertainly of thermal conductivity could be negligible, because the heater is processed by a piece of standard copper. Table 2 summaries the measurement uncertainties. The uncertainty

of the heat flux is 2.02% and the uncertainty of heat transfer coefficient is 2.78%.

5. Experimental result and discussion

5.1 . Boiling heat transfer behaviours of the MWCNTs nanofluid and the deionized water

In order to compare the boiling heat transfer behaviors of the MWCNTs nanofluids to those of the deionized water, experiments of the test fluids were respectively run from single-phase heat transfer to the nucleate boiling under a sub-atmospheric pressure of 1×10^{-3} Pa.

Figure 5(a) shows the instantaneous variation of the boiling surface temperature with the heating time for both the nanofluids with the volume concentration of 0.05% and the base fluid at the heat flux of 740 kW/m^2. Figure 5(b) shows the variation of the heat transfer coefficient with the heating time. At the same heat flux, the boiling curve of the MWCNTs nanofluid is similar to that the base fluid. It can be seen that the boiling surface temperatures of both fluids reduce immediately at the boiling incipience. In the meantime, the heat transfer coefficients increase rapidly after the boiling incipience for both fluids. The boiling heat transfer coefficients gradually increase until reaching the steady state of boiling heat transfer. However, there are some differences boiling behaviors between the MWCNTs nanofluid and the base fluid water. On the one hand, the initial boiling surface temperature of the nanofluids is slightly lower than that of water. It indicates that the boiling incipience of the nanofluids occurs earlier than that of water. On the other hand, the boiling surface temperatures of the nanofluids are much lower than those of water and the transient boiling heat transfer coefficients of the nanofluids are much greater than those of water after reaching steady state boiling.

Figure 6(a) shows the photo of the MWCNTs deposition on the boiling surface. It shows that the nanoparticles are only adhered on the center of copper sheet although the all test section is uniform smooth copper surface. It can be explained by the following reason: nanofluids are composed of solid phase of the nanoparticles and liquid phase of the deionized water. The phase

change of nanofluids is generated on the boiling surface, and the liquid phase is vaporized and divorced from the surface. However, most of the nanoparticles cannot be taken away by the vapor. Therefore, the soild phase is separated from the liquid phase, so the nanoparticles stay on the boiling surface to form agglomerates and gradually produce a deposition. Thus, more and more nanoparticles are deposited on the boiling surface where the center of the copper sheet is.

The result of microscopic photograph by ×80 SEM in Fig. 6(b) shows the rough surface of deposition with pits and bulges. Fig. 6(c) by ×30k SEM proves the point that the deposition is formed by irregular agglomeration of nanotube particles. The surface roughnesses of a copper surface polished by 5000# sandpaper and a nanoparticles surface by 0.05% volume fraction nanofluids deposition were tested using stylus profiler (DektakXT, Bruker, Germany). The copper surface roughness is 20.79 nm and the deposition surface is 4.82 μm. Therefore, the deposition evidently changes the surface roughness of the test section and enhances the boiling heart transfer. This observation agrees to the experimental results by Kole and Dey [30]. They indicated that the surface roughness was influenced by deposition of the nanoparticles.

A static contact angle experiment using deionized water on the smooth surface and the deposition surface was measured by contact angle testing system (OCA15EC, Dataphysics, Germany). As is showed in Fig. 7, the nanoparticles deposition surface decrease 16 degree compared with the copper surface. The variation of contact angle has a great influence on the solid-liquid-vapor interface. Das et al. [31] pointed out that functioned surface could reduce the contact angle to enhance boiling heat transfer. The MWCNTs deposition is conductive to wet the surface, make bubbles easier departure from the boiling surface and increase the boiling heat transfer coefficient. Overall, the main reason of enhanced boiling heat transfer is due to the deposition of agglomerate nanoparticles which may increase the nucleate sites and bubble frequency.

315 *5.2 . The effects of the MWCNTs concentrations and the surfactant on the nucleate boiling heat*
316 *transfer behaviours*

317 Experiments of the boiling heat transfer characteristics of the MWCNTs nanofluid with
318 different volume concentrations from 0.005% to 0.2% without surfactant were conducted at a
319 sub-atmospheric pressure of 1×10^{-3} Pa. First, experiments were conducted at a heat flux of 100
320 kW/m^2 at which the first bubble would generate for the boiling of the deionized water as
321 observed via visualization. Figure 8(a) shows the variation of heat flux versus the superheat
322 degree for the boiling processes with the MWCNTs nanofluid with three volume concentrations
323 of 0.005%, 0.01% and 0.05% and the deionized water at the steady state test conditions. Figure
324 8(b) shows the variation of boiling heat transfer coefficient versus the heat flux for the
325 corresponding test fluids respectively. The experimental results demonstrate that the nanofluids
326 lead to reducing the boiling surface temperatures compared to those of water under the same heat
327 flux. This means that addition of the MWCNTs in the deionized water can enhance the boiling
328 heat transfer. As shown in Fig. 8(b), the heat flux has a significant effect on the boiling heat
329 transfer coefficient. The boiling heat transfer coefficient increases with increasing the heat flux
330 for both the nanofluids and the base fluid. Furthermore, the boiling heat transfer coefficient of
331 the base fluid can be enhanced by adding the MWCNTs in view of boiling curves shifting to the
332 left. It is obvious as indicated that increasing the concentration of the MWCNTs nanofluid may
333 lead to an enhancement of boiling heat transfer. The enhancement increases with increasing the
334 concentration in the present study. The main reason is that increasing concentration of the
335 nanofluid increases the deposition of the nanoparticles on the boiling heat transfer surface and
336 thus increases the nucleation sites and bubble frequency, as such more bubbles may be generated
337 in the boiling process.

338 Figure 9 shows the comparison of the boiling heat transfer coefficient with the MWCNTs
339 volume concentration at a lower heat flux of 100 kW/m^2 and a higher heat flux of 740 kW/m^2.

The heat transfer coefficients at the higher heat flux are around 4 times higher than those at the lower heat flux. The heat transfer coefficient is enhanced with increasing the concentration, although the particle deposition may cause some thermal resistance. Therefore, the thickness of deposition would not be the major factor of HTC in this study. It should be noted that there is a fast-increasing of the nucleate boiling heat transfer coefficients occurred at lower concentrations of the nanofluids. However, this variation of the boiling heat transfer coefficients becomes flat at higher concentrations. It means that this is a critical concentration of the nanofluid at which the boiling heat transfer enhancement remains unchanged beyond this critical concentration. This effect of the nanofluids concentration on the boiling heat transfer coefficient enhancement may be attributed to the variation of the surface roughness due to the nanoparticles deposition. However, there is no significant change with further increasing the concentration of the nanofluid beyond the critical concentration and thus the enhancement of the boiling heat transfer coefficient remains unchanged.

Addition of a surfactant has an important influence on the physical properties of nanofluid such as the surface tension, viscosity, thermal conductivity [32, 33] and the nucleate boiling heat transfer behaviors [34, 35]. In order to understand the effects of various surfactants on the boiling heat transfer behavior in the present study, four different mass concentrations of GA (0.1%, 0.3%, 0.5%, 0.7%) were added into the nanofluid of 0.1% volume concentration of MWCNTs. Figure 10 shows the variation of the boiling heat transfer coefficient with the mass concentration of GA at three different heat fluxes of 520, 630 and 740 kW/m^2. It is obvious that the variations of the heat transfer coefficients clearly indicate that the boiling heat transfer is deteriorated with increasing the concentration of GA in the nanofluids. Furthermore, the heat transfer coefficient curves fall down sharply with increasing the heat flux. It means the negative effect of surfactant GA on the boiling heat transfer becomes more significant at a higher heat flux than those at a lower heat flux.

The conditions of the nanofluids before and after the boiling processes were compared with each other as to understand how the boiling process affects the nanofluid. Figure 11 shows the photographs of the MWCNTs nanofluid before and after boiling processes. Figure 11(a) shows the condition of the prepared nanofluids in all concentrations of GA. The nanofluid is black and the multi-walled carbon nanotube particles are well mixed in the base fluid after ultrasonic oscillation. Figure 11 (b) and (c) shows the condition of the MWCNTs nanofluid after boiling without and with surfactant GA, respectively. The MWCNTs in nanofluid without GA agglomerate and deposit at the bottom of nanofluid after boiling while the nanofluid with surfactant GA still keep good dispersion after boiling process. With increasing heat flux, the activity of nanoparticles is more severe in the liquid, which is helpful to the dispersion of nanoparticles by surfactant. However, the main reason for the enhancement of heat transfer by nanofluid is the aggregation layer of the nanoparticles on the boiling surface. According to this observation, it is obvious that the surfactant can make particles uniformly dispersed in the base fluid and inhibit the deposition generated on the boiling surface, reduce the roughness of boiling surface and weaken the active nucleation sites.

5.3 . The enhancement ratio of boiling heat transfer coefficients of the MWCNTs nanofluid

In order to evaluate the heat transfer enhancement performance, the boiling heat transfer coefficient enhancement ratios of the nanofluids with four different MWCNTs concentrations of 0.005%, 0.01%, 0.05% and 0.1% are compared with each other here. Figure 12 shows the variation of the heat transfer coefficient enhancement ratio versus the heat flux from 100 kW/m^2 to 740 kW/m^2. The maximum heat transfer enhancement ratio is 40.53%. Furthermore, the heat transfer enhancement ratio initially decreases with increasing the heat flux until a value of about 340 kW/m^2 and then increases with increasing the heat flux after this initial decrease. The heat transfer enhancement ratio trends can be explained through the bubble formation and departure behaviors through the visualization of the boiling processes using a high-speed video camera.

In order to observe the variation of bubble formation clearly, boiling experiments of the deionized water were conducted on the surface with deposition. The MWCNTs nanofluid was replaced with the deionized water and the deposition of the MWCNTs was kept on the boiling surface, which was formed by nanofluid with 0.05% concentration after boiling. The bubble generation, growth and departure processes were observed to explain the experimental results and the heat transfer mechanisms.

Figure 13 shows the comparison of the bubble generation processes observed at a low heat flux of 100 kW/m^2 and a high heat flux of 740 kW/m^2 on the boiling surface with the deposition of the MWCNTs. As shown in Fig. 13(a), a bubble emerges on the boiling surface and kept growing. At low pressure, the superheated liquid is full around the bubbles because of the low boiling point of working fluid. On the one hand, with the bubble rising, the bubble volume increases with the increase of the pressure. On the other hand, the bubble dramatically becomes large because the water around the bubble continually vaporizes into the bubble. Shortly afterwards, it departures from the surface slowly which may deteriorate the heat transfer from the boiling surface to the fluid. The vapor condenses rapidly after contacting the upper copper surface. At last, the liquid back to initial state without phase-change.

As mentioned in the fore-going, the deposition of the nanoparticles on the boiling surface evidently improves the number of nucleation sites and contact angle which can increase and reduce the region of no phase-change. The slower generation and departure of bubble, the more obvious enhancement of heat transfer of deposition. At lower heat flux, the increase of the bubble formation rate is the most important mechanism to enhanced heat transfer by nanofluids. But with increasing the heat flux, the bubble formation rate also increases, hence heat transfer enhancement of nanofluids with increasing heat flux becomes weak. As observed in Fig. 12, this transitional heat flux is around 340 kW/m^2 where the bubbles become continuous. Thus the boiling heat transfer coefficient enhancement ratios continue to decline from 100 to 340 kW/m^2

heat fluxes.

The different boiling patterns at a higher heat flux are shown in Fig. 13(b). It shows that more than one bubble generated from the boiling surface and grew bigger rapidly, and then the bubbles departure becomes fast. New bubbles generated immediately when the previous bubbles just left and the heat transfer becomes stable. Shoghl et al. [20] proposed the effect of both deposition surface and properties of nanofluids influenced the boiling heat transfer coefficient. The enhanced heat transfer mechanisms at high heat fluxes are attributed to not only the increase of the nucleation site density but also the disturbance of particles in fluid. In this study, the experimental results also show that the enhancement ratio of boiling heat transfer coefficient can be increased by improving the effect of deposition and degree of particle disturbance with increasing heat flux at high heat fluxes from 340 to 740 kW/m^2.

6. Conclusions

In the present study, first, stable and uniform nanofluid preparation technology is introduced. Then, experiments of nucleate boiling heat transfer characteristics of the MWCNT water-based nanofluids and the base fluid deionized water in a confined space were conducted at a sub-atmospheric pressure of 1×10^{-3} Pa and heat fluxes from 100 to 740 kW/m^2. The uncertainty of the heat flux is 2.02% and the uncertainty of heat transfer coefficient is 2.78%. The roughness and contact angle of the deposited layer and copper surface were compared. The effects of the concentrations of nanoparticles and surfactants on the boiling heat transfer behaviors have been analyzed. The bubble generation and departure characteristics together with the observed particle deposition on the boiling heat transfer surface have been used to explain the experimental results and the heat transfer enhancement mechanisms. The effects of heat flux on the heat transfer enhancement have also been discussed. From the present study, the following conclusions have been reached:

(1) Stable and uniform water-based MWCNTs nanofluid can be produced using the two steps method with addition of GA.

(2) Compared with the base fluid, the MWCNTs nanofluid can enhance boiling heat transfer. The maximum heat transfer enhancement can reach 40.53%. The main reason of the heat transfer enhancement is due to the deposition of the MWCNTs on the boiling surface which can increase the roughness and reduce the contact angle.

(3) The boiling heat transfer coefficient increases with increasing concentration of the MWCNTs nanofluids owing to increasing nucleation sites of boiling surface and bubble formation rate. A critical volume concentration was found where the boiling heat transfer coefficient will not be further enhanced. In general, it is limited to enhance the boiling heat transfer coefficient by nanofluids because further deposition of the nanoparticles won't obviously improve the boiling surface.

(4) Addition a surfactant may keep the stable and uniform of the MWCNTs nanofluid. However, it seems that the surfactant has a negative effect on the boiling heat transfer in the present study. Addition of GA inhibits the formation of deposition and thus weakens the boiling heat transfer of the nanofluid. The higher the concentration of GA, the worse the boiling heat transfer is.

(5) The heat flux has a significant effect on the boiling heat transfer ratio. The boiling heat transfer enhancement ratio decreases with increasing the heat flux when the heat flux is less than 340 W/m^2 while it increases with increasing the heat flux beyond this value.

(6) The mechanisms of the boiling heat transfer enhancement of the MWCNTs nanofluid are quite different for the lower and higher heat fluxes. At the low heat fluxes, the deposition layer increases the bubble formation frequency, and substantially strengthens the boiling heat transfer. At the high heat fluxes, the increase of nanoparticles concentration and heat flux enhances particle disturbance in fluid. Besides, with the enhancement of deposition and

particle disturbance, the enhancement ratio of boiling heat transfer coefficient is evidently increased.

Acknowledgements

This work is supported by a research fund of the National Natural Science Foundation of China (No. 51576005).

References

[1] S.U.S. Choi, Enhancing thermal conductivity of fluids with nanoparticles, Developments and Application of Non-newtonian Flows, ASME 66 (1995) 99-105.

[2] Y.M. Xuan, Q. Li, W.F. Hu, Aggregation structure and thermal conductivity of nanofluids, AIChE J. 49 (4) (2003) 1038-1043.

[3] M.J. Assael, C.F. Chen, I. Metaxa, W.A. Wakeham, Thermal Conductivity of Suspensions of Carbon Nanotubes in Water, Int. J. Thermophys. 25 (4) (2004) 971-985.

[4] S.A. Angayarkanni, J. Philip, Review on thermal properties of nanofluids: Recent developments, Adv. Colloid Interface Sci. 225 (2015) 146-176.

[5] M. Raja, R. Vijayan, P. Dineshkumar, M. Venkatesan, Review on nanofluids characterization, heat transfer characteristics and applications, Renew. Sust. Energ. Rev. 64 (2006) 163-173.

[6] Y.J. Hwang, Y.C. Ahn, H.S. Shin, C.G. Lee, G.T. Kim, H.S. Park, J.K. Lee, Investigation on characteristics of thermal conductivity enhancement of nanofluids, Curr. Appl. Phys. 6 (2006) 1068-1071.

[7] L. Cheng, L. Liu, Boiling and two-phase flow phenomena of refrigerant-based nanofluids: Fundamentals, applications and challenges, Int. J. Refrig. 36 (2) (2013) 421-446.

[8] L. Cheng, E.P. Bandarra Filho, J.R. Thome, Nanofluid two-phase flow and thermal physics: A new research frontier of nanotechnology and its challenges, J. Nanosci. Nanotech. 8 (2008) 3315-3332.

[9] G.D. Xia, R. Liu, J. Wang, M. Du, The characteristics of convective heat transfer in microchannel heat sinks using Al_2O_3 and TiO_2 nanofluids, Int. Commun. Heat Mass Transf. 76 (2016) 256-264.

[10] D. Yadav, J Wang, R Bhargava, J Lee, H.H. Cho, Numerical investigation of the effect of magnetic field on the onset of nanofluid convection, Appl. Therm. Eng. 103 (2016) 1441-1449.

[11] D. Ciloglu, A. Bolukbasi, A comprehensive review on pool boiling of nanofluids, Appl. Therm. Eng. 84 (2015) 45-63.

[12] R. Kamatchi, S. Venkatachalapathy, Parametric study of pool boiling heat transfer with nanofluids fortheenhancement of critical heat flux: A review, Int. J. Therm. Sci. 87 (2015) 228-240.

[13] X.D. Fang, Y.F. Chen, H.L. Zhang, W.W. Chen, A.Q. Dong, R. Wang, Heat transfer and critical heat flux of nanofluid boiling: A comprehensive review, Renew. Sust. Energ. Rev. 62 (2016) 924-940.

[14] Y.M. Yang, J.R. Maa, Boiling of suspension of solid particles in water, Int. J. Heat Mass Transf. 27 (1984) 145-147.

[15] H.S. Xue, J.R. Fan, R.H. Hong, Y.C. HU, Characteristic boiling curve of carbon nanotube nanofluid as determined by the transient calorimeter technique, Appl. Phys. Lett. 90 (90) (2007) 99-105.

[16] A. Amiri, M. Shanbedi, H. Amiri, S. Zeinali Heris, S.N. Kazi, et al, Pool boiling heat transfer of CNT/water nanofluids, Appl. Therm. Eng. 71 (71) (2014) 450–459.

[17] M.M. Sarafraz, F. Hormozi, Nucleate pool boiling heat transfer characteristics of dilute

Al_2O_3–ethyleneglycol nanofluids, Int. Commun. Heat Mass Transf. 58 (2014) 96-104.

[18] M.M. Sarafraz, F. Hormozi, Experimental investigation on the pool boiling heat transfer to aqueous multi-walled carbon nanotube nanofluids on the micro-finned surfaces, Int. J. Therm. Sci. 100 (22) (2015) 255-266.

[19] M.M. Sarafraz, F. Hormozi, S.M. Peyghambarzadeh, Pool boiling heat transfer to aqueous alumina nano-fluids on the plain and concentric circular micro-structured (CCM) surfaces, Exp. Therm. Fluid Sci. 72 (2016) 125-139.

[20] S.N. Shoghl, M. Bahrami, M. Jamialahmadi, The Boiling Performance of ZnO, α-Al_2O_3 and MWCNTs-Water Nanofluids: An Experimental Study, Exp. Therm. Fluid Sci. 80 (2016) 27-39.

[21] C.M. Rops, R. Lindken, J.F.M. Velthuis, J. Westerweel, Enhanced heat transfer in confined pool boiling, Int. J. Heat Fluid Flow 30 (4) (2009) 751-760.

[22] G.M. Zhang, Z.L. Liu, C. Wang, An experimental study of boiling and condensation co-existing phase change heat transfer in small confined space, Int. J. Heat Mass Transf. 64 (2) (2013) 1082-1090.

[23] C.F. Liu, C.Y. Yang, Effect of space distance for boiling heat transfer on micro porous coated surface in confined space, Exp. Therm. Fluid Sci. 50 (10) (2013) 163-171.

[24] A. Ghozatloo, A.M. Rashidi, M. Shariaty-Niasar, Effects of surface modification on the dispersion and thermal conductivity of CNT-water nanofluids, Int. Commun. Heat Mass Transf. 54 (46) (2014) 304-310.

[25] M. Farbod, A. Ahangarpour, S.G. Etemad, Stability and thermal conductivity of water-based carbon nanotube nanofluids, PARTICUOLOGY 22 (5) (2015) 59-65.

[26] W.S. Sarsam, A. Amiri, S.N. Kazi, A.Badarudin, Stability and thermophysical properties of non-covalently functionalized graphene nanoplatelets nanofluids, Energy Convers. Manage. 116 (2016) 101-111.

[27] D.K. Devendira, V.A. Amirtham, A review on preparation, characterization, properties and applications of nanofluids, Renew. Sust. Energ. Rev. 60 (2016) 21-40.

[28] M.N.A.W.M. Yazid, N.A.C. Sidik, R. Mamat, G. Najafi, A review of the impact of preparation on stability of carbon nanotube nanofluids, Int. Commun. Heat Mass Transf. 78 (2016) 253-263.

[29] S.J. Kline, F.A. McClintock, Describing Uncertainties in Single-Sample Experiments, Mech. Eng. 75 (1) (1953) 3-8.

[30] M. Kole, T.K. Dey, Investigations on the pool boiling heat transfer and critical heat flux of ZnO-ethylene glycol nanofluids, Appl. Therm. Eng. 37 (16) (2012) 112-119.

[31] S. Das, B. Saha, S. Bhaumik, Experimental study of nucleate pool boiling heat transfer of water by surface functionalization with SiO_2 nanostructure, Exp. Therm. Fluid Sci. 81 (2016) 454-465.

[32] M.Z. Zhou, G.D. Xia, J. Li, L. Chai, L.J. Zhou, Analysis of factors influencing thermal conductivity and viscosity in different kinds of surfactant solutions, Exp. Therm. Fluid Sci. 36 (2012) 22-29.

[33] G.D. Xia, H.M. Jiang, R. Liu, Y.L. Zhai, Effects of surfactant on the stability and thermal conductivity of Al2O3-deionized water nanofluids, Int. J. Therm. Sci. 48 (2014) 118-124.

[34] L. Cheng, D. Mewes, A. Luke, Boiling phenomena with surfactants and polymeric additives: A state-of-the-art review, Int. J. Heat Mass Transf. 50 (13-14) (2007) 2744-2771.

[35] A. Najim, V. More, A. Thorat, S. Patil, S. Savale, Enhancement of pool boiling heat transfer using innovative non-ionic surfactant on a wire heater, Exp. Therm. Fluid Sci. 82 (2017) 375-380.

Nomenclatures

h	heat transfer coefficient, W/ m^2·K
q	heat flux, W/m^2
T	temperature, K
z	distance between two temperature measurement points, m

Greek symbols

λ	thermal conductivity, W/ m·K
η	enhancement ratio of boiling heat transfer coefficient, %

Subscripts

f	working fluid
w	boiling surface
nf	nanofluids
dw	deionized water

Abbreviations

GA	gum acacia
MWCNTs	multi-walled carbon nanotubes
SEM	scanning electron microscopy
TEM	transmission electron microscopy

List of Table and Figure Captions

Fig. 13. Photographs of the bubble generation, growth and departure on the boiling surface with the MWCNTs deposition at two heat fluxes: (a) 100kW/m^2 and (b) 740kW/m^2.

Table 1

Parameters of the multi-walled carbon nanotube nanoparticles.

Outer diameter(nm)	Inner diameter(nm)	Length (μm)	Purity	Density (g/cm^3)	Specific surface area(m^2/g)
10-20	5-10	10-30	>98%	2.1	200

Table 2

The summary of measurement uncertainties.

Parameter	Unit	Uncertainty
Temperature	K	± 0.1
Distance between thermal couples	mm	± 0.1
Voltage	V	± 0.1
Current	A	±0.025
Pressure	Pa	0.25%
Heat flux	W/m^2	2.02%
Heat transfer coefficient	$W/ m^2 \cdot K$	2.78%

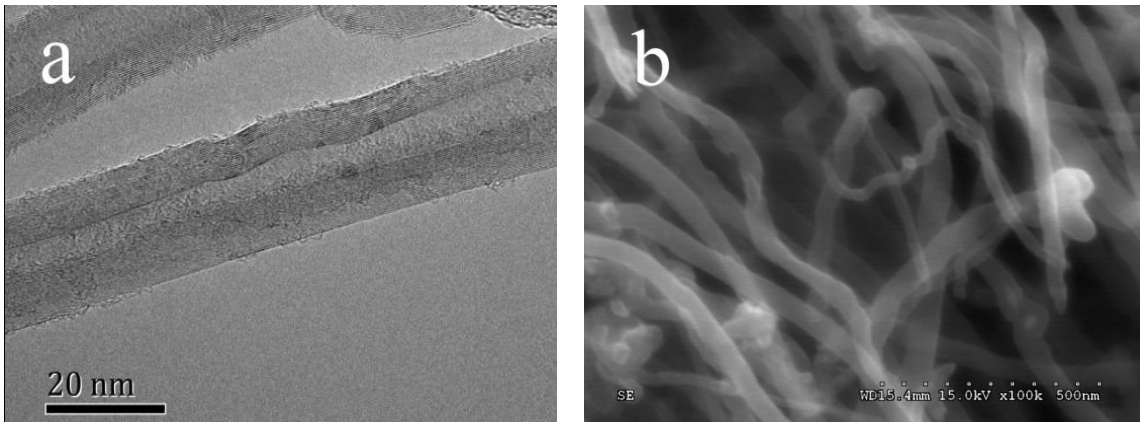

Fig. 1. Microscopic photograph of the MWCNTs by (a) TEM and (b) SEM .

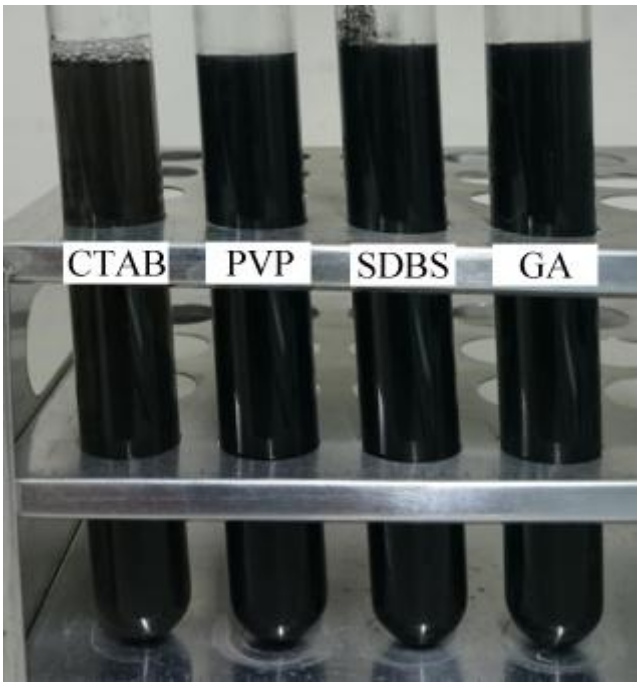

(a) Fresh prepared nanofluids.

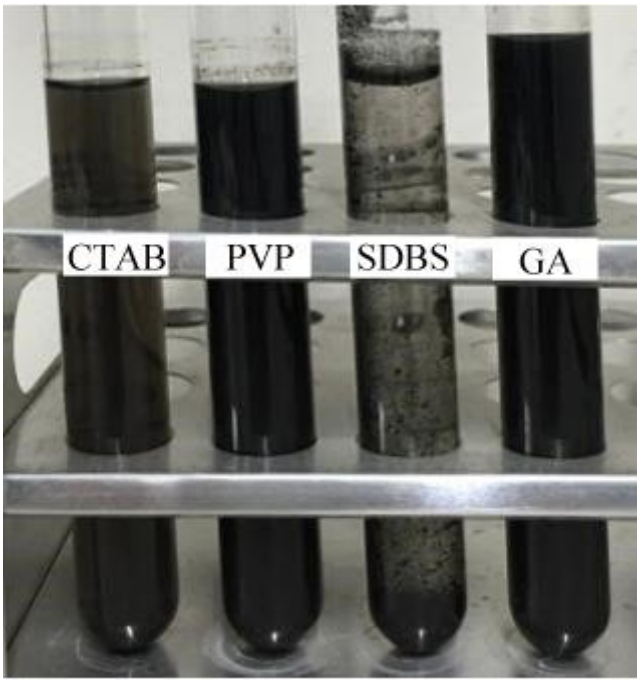

(b) Nanofluids after standing for three months.

Fig. 2. The images of the dispersed MWCNTs nanofluids with four different surfactants: (a) Fresh prepared nanofluids and (b) Nanofluids after standing for three months.

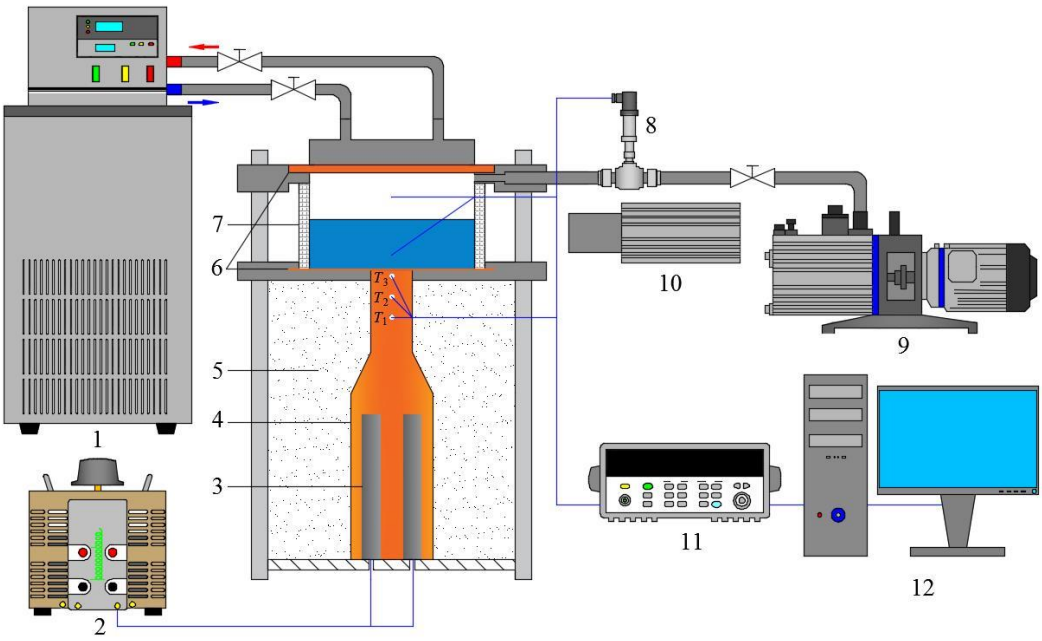

Fig. 3. Schematic diagram of the experimental rig.

(1) Thermostatic water container, (2) Voltage regulator, (3) Cartridge heater, (4) Copper rod, (5) Insulation layer, (6) Copper sheet, (7) Quartz window (8) Pressure gauge, (9) Vacuum pump, (10) High-speed camera, (11) Data acquisition instrument, (12) PC.

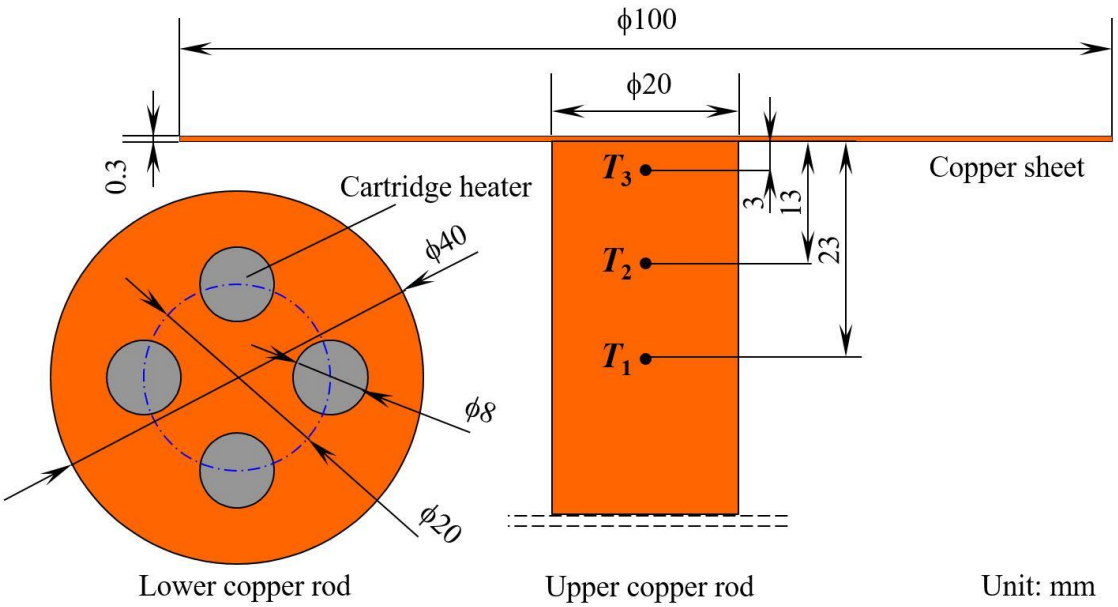

Fig. 4. Schematic diagram of the test section and the heating arrangement.

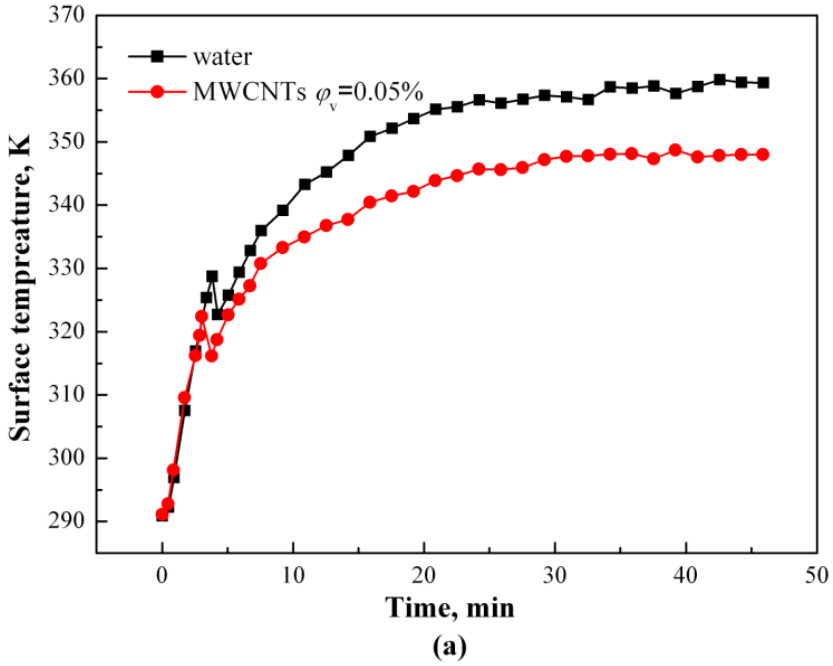

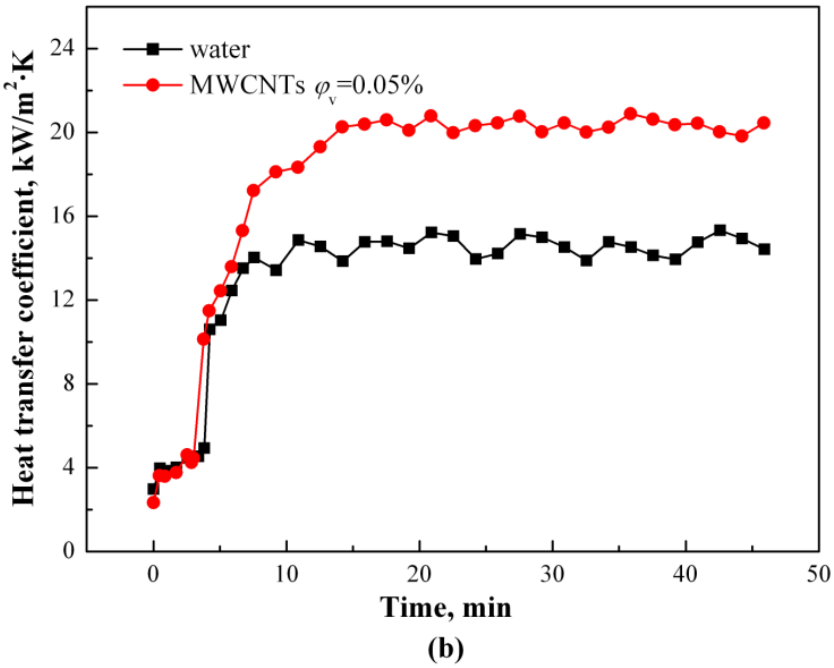

Fig. 5. Boiling curves of the MWCNTs nanofluid with a volume concentration of 0.05% and deionized water: (a) Boiling surface temperature vs. time; (b) Boiling heat transfer coefficient vs. time.

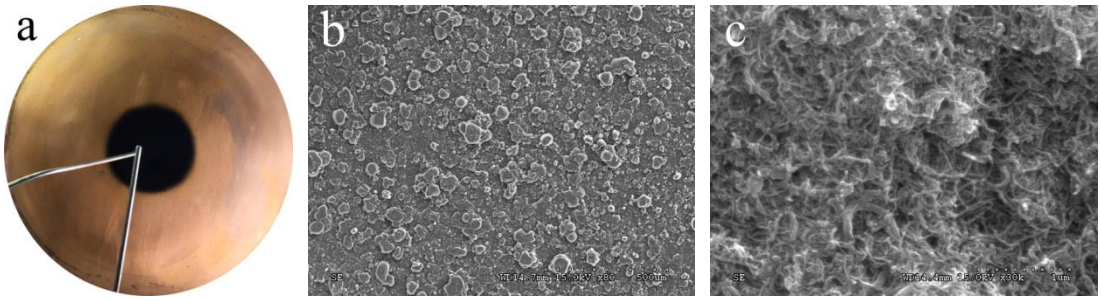

Fig. 6. Macroscopic and microscopic photographs of nanoparticles deposition: (a) by camera, (b) by ×80 SEM, (c) by ×30k SEM.

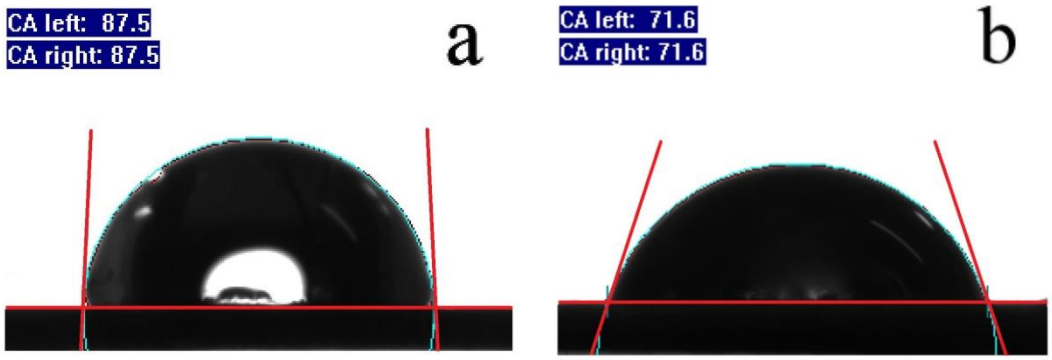

Fig. 7. Static contact angle of (a) a smooth copper surface and (b) a nanoparticles deposition surface.

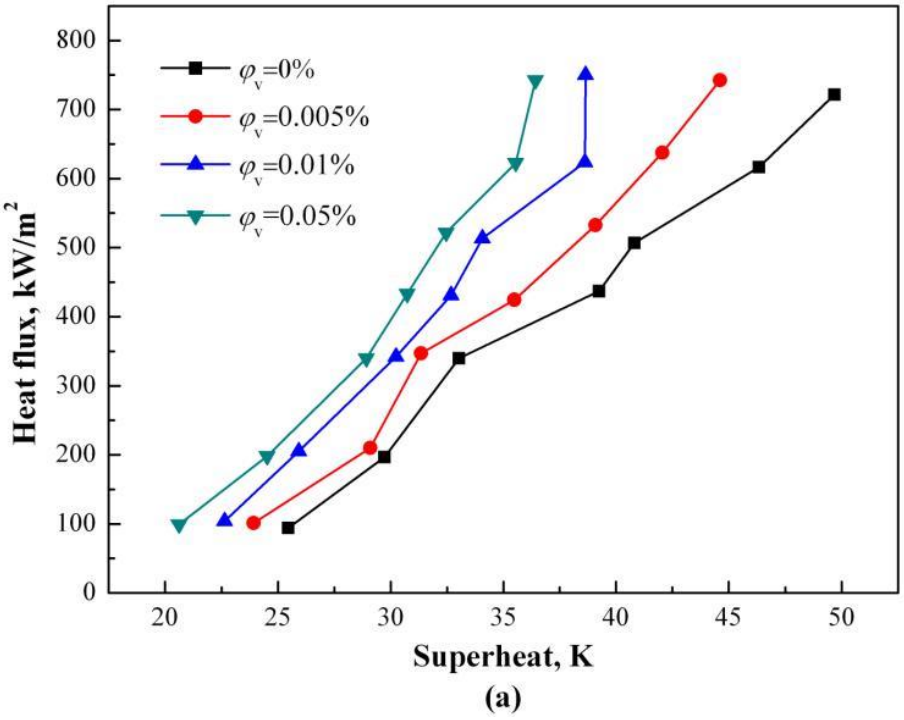

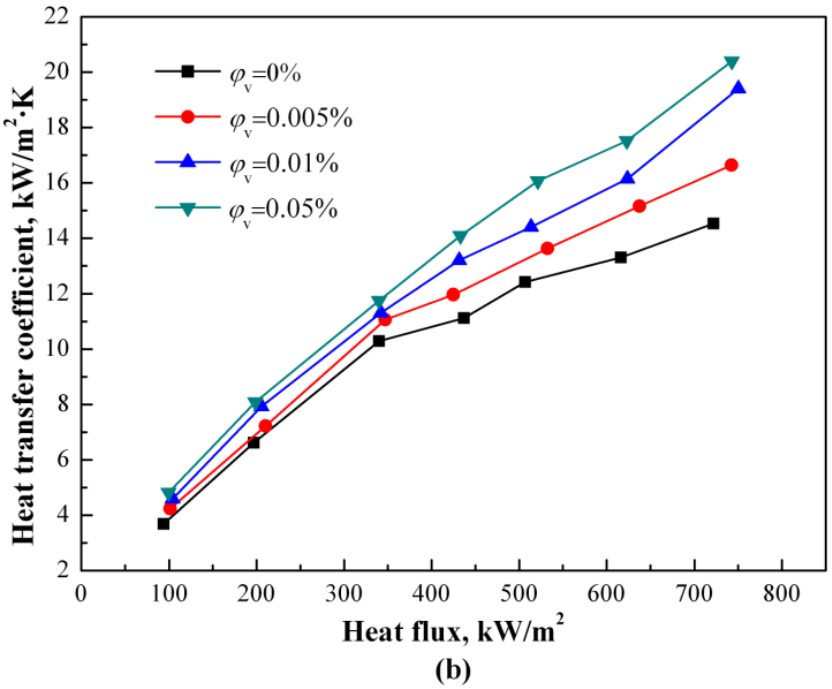

Fig. 8. Boiling curves of the MWCNTs nanofluids with three different volume concentrations of 0.005%, 0.01% and 0.05%, and the deionized water: (a) Heat flux vs. superheat degree, (b) Boiling heat transfer coefficient vs. heat flux.

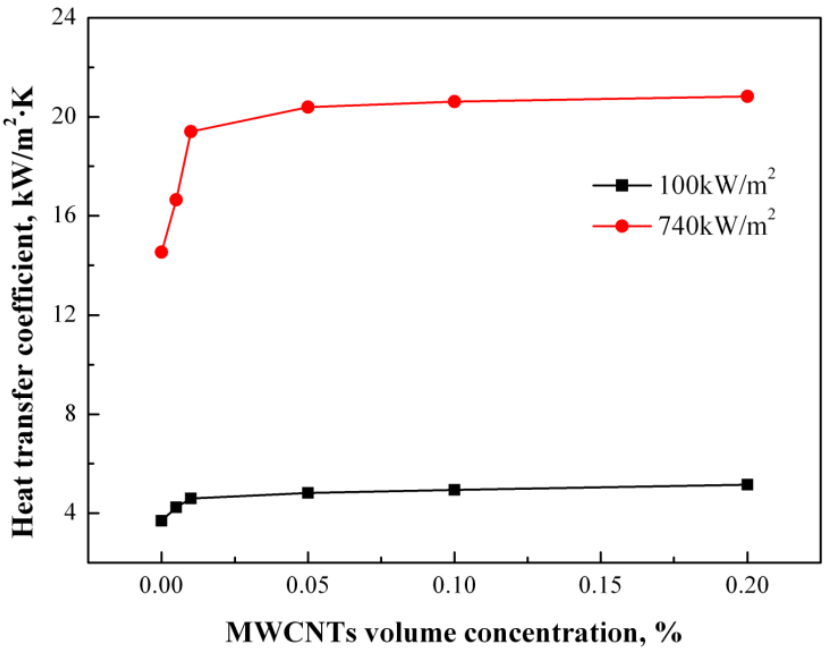

Fig. 9. Variation of the boiling heat transfer coefficients of the MWCNTs nanofluids with the concentrations at two different heat fluxes of 100 kW/m^2 and 740 kW/m^2.

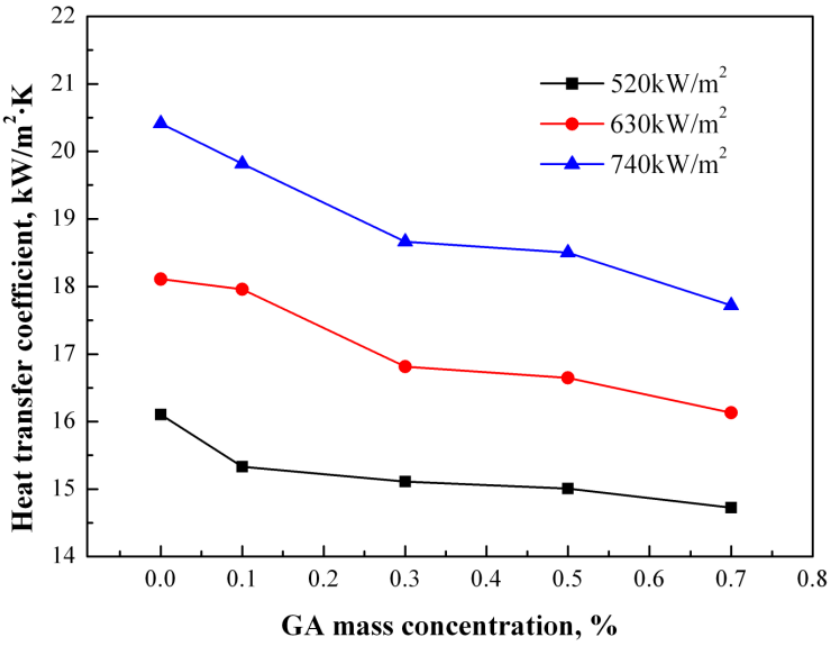

Fig. 10. Variation of the boiling heat transfer coefficient with the mass concentration of surfactant GA at three different heat fluxes of 520 kW/m^2, 630 kW/m^2 and 740 kW/m^2.

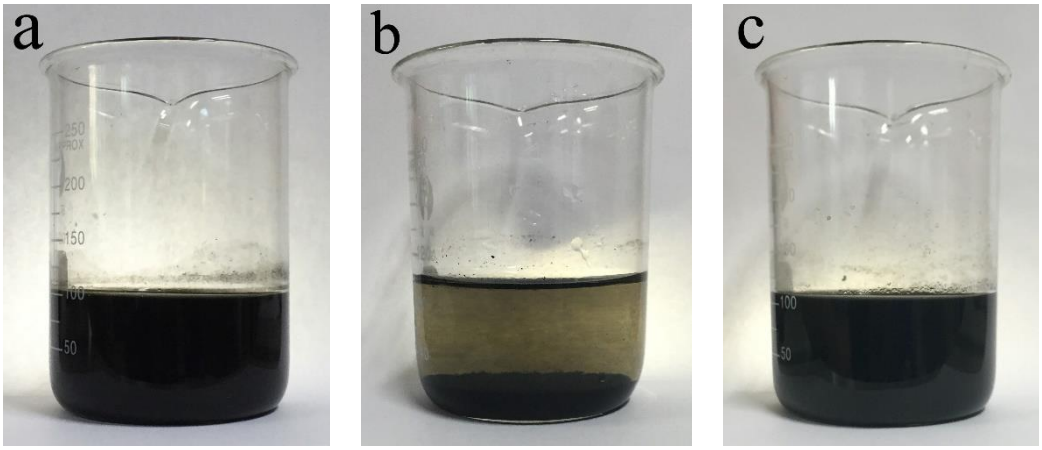

Fig. 11. Agglomeration condition of the MWCNTs nanofluids: (a) before boiling, (b) without GA after boiling, (c) with GA after boiling.

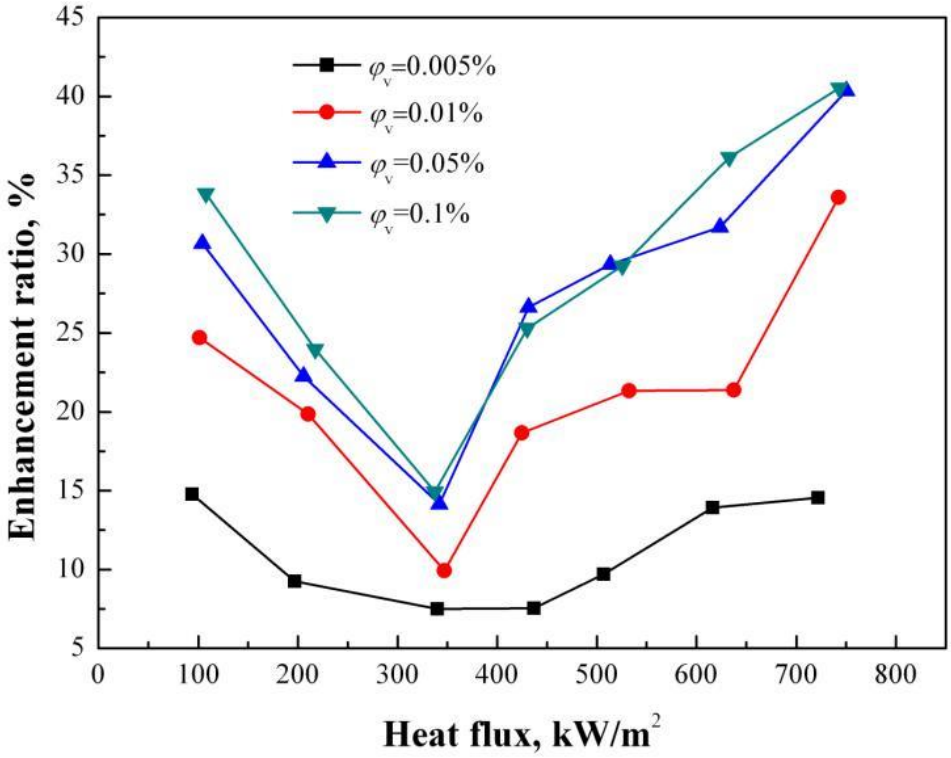

Fig. 12. Variation of the boiling heat transfer coefficient enhancement ratios of the MWCNTs nanofluids with the heat flux for four different volume fractions of 0.005%, 0.01%, 0.05% and 0.1%.

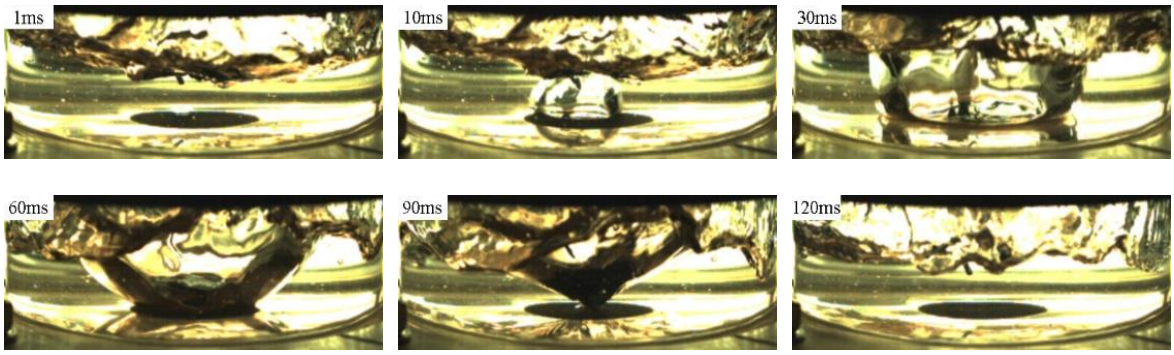

(a)

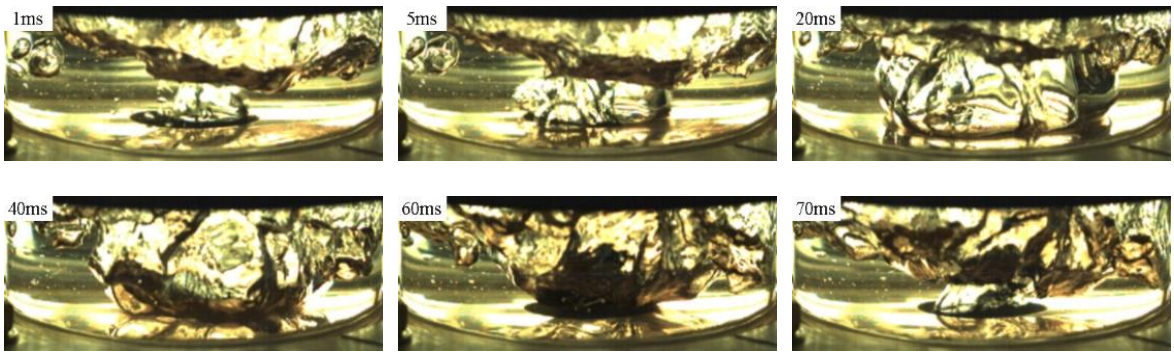

(b)

Fig. 13. Photographs of the bubble generation, growth and departure on the boiling surface with the MWCNTs deposition at two heat fluxes: (a) 100kW/m^2 and (b) 740kW/m^2.